Control Characteristics of High-Voltage Resonant DC/DC Converter

Nikolay Bankov[1], Yasen Madankov[2] and Aleksandar Vuchev[3]

Abstract – **A state plane analysis of high-voltage resonant DC/DC converter, operating above the resonant frequency, is presented. The parasitic parameters of the matching transformer are taken into account during the study. The possible operating modes of the converter are defined, according to the commutation time of the rectifier diodes. The control characteristics are obtained. In the plane of these characteristics the boundary curve between the particular modes is shown, as well as the area of soft commutation of the transistors. The results from the analysis are compared with these from computer simulations of the converter with OrCAD PSpice.**

Keywords – **High-voltage resonant DC/DC converter, Control characteristics**

I. INTRODUCTION

The resonant DC/DC converters have been proved as a proper choice in the high-voltage power supplies design [1], [2]. The LCC topology is one of the most suitable for these applications [2]÷[4]. One of the reasons is the possibility of operation in the whole loading range – from no-load to short circuit, preserving the soft commutation conditions of the switching devices. Another important advantage of these converters is the opportunity to implement the high-voltage matching transformer parasitic parameters (leakage inductance and winding capacitance) in the resonant tank [4].

The rectifier diodes commutations are not instantaneous, because of the capacitance which is parallel to the input of the rectifier. Usually this circumstance is neglected [5]. A study of the possible operating modes of LCC resonant DC/DC converter is proposed in [6] and [7], where the transformer's parasitic parameters are taken into account. As a result the output characteristics of the converter are obtained.

The aim of the present paper is to extend the analysis for the control characteristics area of the LCC resonant DC/DC converter. The boundary curve between the operating modes and the region of soft commutation of the transistors are obtained as an addition. An OrCAD PSpice simulation is used to achieve accuracy verification of the proposed analysis.

[1]Nikolay Bankov is with the Department of Electrical Engineering and Electronics, Technical Faculty, University of Food Technologies, 26 Maritza Blvd., 4002 Plovdiv, Bulgaria, E-mail: nikolay_bankov@yahoo.com

[2]Yasen Madankov is with the Department of Electrical Engineering and Electronics, Technical Faculty, University of Food Technologies, 26 Maritza Blvd., 4002 Plovdiv, Bulgaria, E-mail: yasen.madankov@gmail.com

[3]Aleksandar Vuchev is with the Department of Electrical Engineering and Electronics, Technical Faculty, University of Food Technologies, 26 Maritza Blvd., 4002 Plovdiv, Bulgaria, E-mail: avuchev@yahoo.com

II. CONVERTER OPERATING MODES

The circuit of the considered resonant converter is shown on Fig. 1. It consists of full-bridge inverter (transistors $Q_1 \div Q_4$ with freewheeling diodes $D_1 \div D_4$), resonant circuit (L, L_T, C and C_T), high-voltage transformer (Tr) and uncontrollable full-bridge rectifier ($D_5 \div D_8$). Snubber capacitors ($C_1 \div C_4$), which provide zero voltage switching (ZVS), are connected in parallel with the transistors. Filter capacitors (C_{F1} and C_{F2}) are connected to both the input and output of the converter.

The output power control is achieved by a change of the operating frequency, which is higher than the resonant one.

All circuit elements (without the matching transformer) are assumed to be ideal; the input and output voltage ripples are neglected, as well as the influence of the snubbers.

The transformer is shown on Fig. 1 with its simplified equivalent circuit, provided that the magnetizing current of each transformer is negligible to the resonant tank current. In such case Tr is comprised by its full leakage inductance L_T and the windings capacitance C_T, referred to the primary side, as well as an ideal transformer with turns ratio k.

The leakage inductance L_T is connected in series with the inductance of the resonant circuit L and can be regarded as part of it. With the capacitances C_T the resonant tank becomes of third order (L, C and C_T).

The inverter's output voltage (u_a) polarity changes immediately, because the snubber capacitors are not taken into account. But the presence of capacitance C_T makes the commutations in the input voltage of the rectifier (u_b) non-instantaneous. They start when a diode pair (D_5/D_7 or D_6/D_8) stops conducting at the moments of zeroing the current through the resonant circuit (i) and end up when the other diode pair (D_6/D_8 or D_5/D_7) starts conducting, while the capacitor C_T recharges from $+U_0/k$ to $-U_0/k$ or backwards. During these commutations none of the rectifier diodes conducts and the resonant current flows through the capacitance C_T.

When the load and/or the switching frequency are deeply changed, two different operating modes of the converter could be observed.

Characteristic of the first one is that the commutations in the rectifier occur entirely in the conducting intervals of the transistors. This is the *main* operating mode of the converter and is observed at comparatively small values of the load resistor R_0.

We have the second case when the converter is very close to no-load regime. Than the commutations in the rectifier complete after these of the inverter, i.e. the rectifier diodes

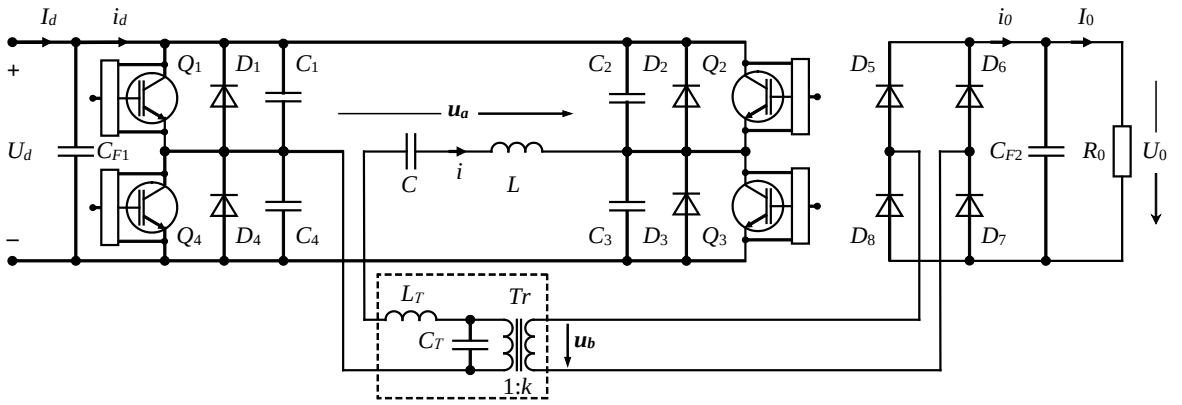

Fig. 1. Scheme of the high-voltage resonant DC/DC converter

start conducting after the corresponding inverter diodes are forward-biased. This mode is called *boundary*.

III. State Plane Analysis

All parameters are presented in relative units, as follow:

$U'_{Cm} = U_{Cm}/U_d$ - peak value of the voltage drop across the capacitor *C*;

$U'_0 = \dfrac{U_0}{k.U_d}$ - output voltage;

$I'_0 = \dfrac{k.Z_0}{U_d}.I_0$ - output current;

$\nu = \omega/\omega_0$ - normalized switching frequency

where ω is the operating frequency of the converter, $\omega_0 = 1/\sqrt{LC}$ is the resonant frequency and $Z_0 = \sqrt{L/C}$ is the characteristic impedance of the resonant tank *L*-*C*. Coefficients $a = C_T/C$ and $n = \sqrt{(a+1)/a}$ are also used.

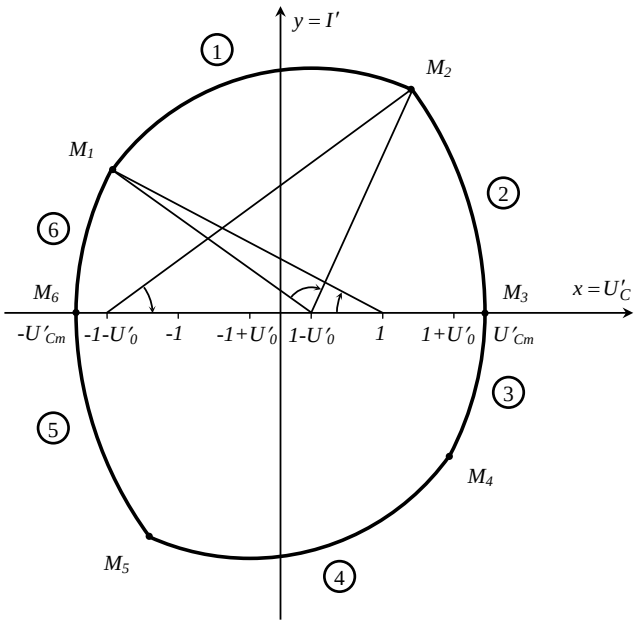

Fig. 2. State plane trajectory for the *main* operating mode

The normalized load resistance is expressed as:

$$R'_0 = U'_0/I'_0 = R_0/k^2 Z_0 \qquad (1)$$

As proposed in [6], the work of the converter in the *main* operating mode could be illustrated by a state plane trajectory with axes $(x = U'_C; y = I')$, shown on Fig. 2. Each operating period is divided into six consecutive intervals: **1**, **3**, **4** and **6** – conduction of transistors, **2** and **5** – conduction of the inverter reverse diodes, **3** and **6** – rectifier diodes commutation.

The times of these intervals for half a period could be expressed using the coordinates of points M_1, M_2 and the resonant frequency ω_0, by Eqs. (2)÷(7). Note that for t_3 (commutation time of the rectifier diodes) *C* and C_T are connected in series. Thus the resonant frequency is $\omega'_0 = n\,\omega_0 = 1/\sqrt{LC_E}$, where $C_E = C.C_T/(C + C_T)$.

$$t_1 = \frac{1}{\omega_0}\left(arctg\frac{y_2}{-x_2+1-U'_0} - arctg\frac{y_1}{-x_1+1-U'_0}\right) \qquad (2)$$

for $x_2 \le 1-U'_0$ and $x_1 \le 1-U'_0$

$$t_1 = \frac{1}{\omega_0}\left(\pi - arctg\frac{y_2}{x_2-1+U'_0} - arctg\frac{y_1}{-x_1+1-U'_0}\right) \qquad (3)$$

for $x_2 > 1-U'_0$ and $x_1 \le 1-U'_0$

$$t_1 = \frac{1}{\omega_0}\left(arctg\frac{y_2}{-x_2+1-U'_0} + arctg\frac{y_1}{x_1-1+U'_0}\right) \qquad (4)$$

for $x_2 > 1-U'_0$ and $x_1 > 1-U'_0$

$$t_2 = \frac{1}{\omega_0} arctg\frac{y_2}{x_2+1+U'_0} \qquad (5)$$

$$t_3 = \frac{1}{n\omega_0}\left(arctg\frac{ny_1}{-x_1+1-U'_0}\right) \quad \text{for } x_1 \le 1-U'_0 \qquad (6)$$

$$t_3 = \frac{1}{n\omega_0}\left(\pi - arctg\frac{ny_1}{x_1-1+U'_0}\right) \quad \text{for } x_1 \ge 1-U'_0 \qquad (7)$$

The used coordinates represent the initial values of the resonant current (y_i) and the voltage drop across the capacitor C (x_i) for the particular interval (in relative units):

$$x_1 = -U'_{Cm} + 2aU'_0 \tag{8}$$

$$y_1 = \sqrt{4aU'_0\left(U'_{Cm} - aU'_0 + 1\right)} \tag{9}$$

$$x_2 = U'_0 U'_{Cm} - aU'^2_0 \tag{10}$$

$$y_2 = \sqrt{U'_{Cm}\left(U'_{Cm} + 2\right)\left(1 - U'^2_0\right) + aU'^2_0\left(2 + 2U'_0 + 2U'_0 U'_{Cm} - aU'^2_0\right)} \tag{11}$$

The equation for the output current of series resonant converter is known [8]: $I'_0 = 2\nu U'_{Cm}/\pi$. But in this case, $I'_0 = 0$ during the commutations in the rectifier, because of the persistence of the parallel capacitance C_T, so the value is:

$$I'_0 = 2\nu U'_{Cm}/\pi - \Delta I'_0 = 2\nu\left(U'_{Cm} - aU'_0\right)/\pi \tag{12}$$

The way for determination of the coordinates of the points M_i and the time intervals ($t_1 \div t_3$) for the *boundary* operating mode of the converter is quite similar. Detailed analysis for this case is given in [7].

IV. Control Characteristics and Boundary Curves

Using Eqs. (1) and (12), U'_{Cm} can be submitted in function of U'_0, ν, R'_0 и a:

$$U'_{Cm} = \frac{\pi}{2\nu} \cdot \frac{U'_0}{R'_0} + aU'_0 \tag{13}$$

By Eq. (13) U'_{Cm} is eliminated from Eqs. (8)÷(11). Next steps are consecutive substitution of Eqs. (8)÷(11) in Eqs. (2) ÷(7) and after that Eqs. (2)÷(7) in:

$$\frac{\pi}{\nu} = \omega_0\left(t_1 + t_2 + t_3\right) \tag{14}$$

Solving Eq. (14), a function $U'_0 = f\left(a, \nu, R'_0\right)$, which represents the control characteristics of the converter for the *main* operating mode, could be obtained. The procedure for the *boundary* mode is the same, only the equations for (x_i; y_i) and t_i have to be used from [7].

The control characteristics of LCC resonant DC/DC converter with capacitors ratio $a = 1,0$, for different values of R'_0, are shown on Fig. 3. Dashed curves correspond to the *boundary* mode and continuous – for the *main* mode.

In the *main* operating mode the rectifier commutations (intervals **3** and **6**) have to complete before the inverter commutations begin. This is true if the statement $x_1 \le x_2$ is fulfilled. Expressed by Eqs. (8), (10) and (13), the next inequality is received:

$$\nu \le \frac{\pi}{2a} \cdot \frac{U'_0 + 1}{R'_0} \tag{15}$$

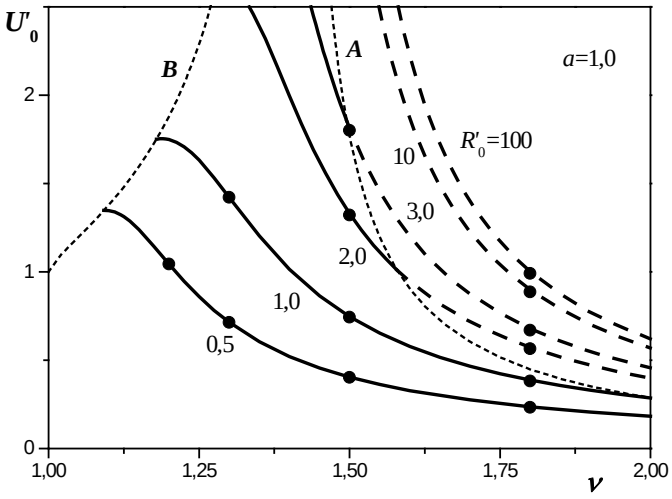

Fig. 3. Control characteristics of LCC resonant DC/DC converter

To ensure the soft switch-on of the transistors at zero voltage (ZVS), the inverter commutations (points M_2 and M_5) have to complete before zero crossing of the resonant current. If this is not fulfilled, the switching-off of one the transistor pairs doesn't lead to soft switch-on of the other pair at zero voltage and the converter stops working. This is covered by the statement $x_2 < U'_{Cm}$, which expressed by Eqs. (10) and (13) leads to the inequality:

$$\nu \le \frac{\pi}{2a} \cdot \frac{U'_0 - 1}{R'_0} \tag{16}$$

Eqs. (15) and (16) provide the possibility to plot the boundary curve between the *main* and the *boundary* modes (curve **A**) in the control characteristics plane (Fig. 3), as well as the curve of the soft commutation (curve **B**). These curves define the area of each operating mode of the converter.

V. Simulating Results

In order to prove the obtained theoretical results a transistor LCC resonant DC/DC converter, operating above the resonant frequency, was designed using the methodology proposed in [9]. Its input parameters are:

- output power $P_0 = 3\,kW$;
- output voltage $U_0 = 150\,V$;
- operating frequency $f = 100\,kHz$;
- supply voltage $U_d = 300\,V$;
- $a = 1,0$; $k = 1$.

The chosen nominal operating point is at $\nu = 1,15$. Than the following values for the elements of the resonant tank are obtained: $L = 72,577\ \mu H$; $C = 46,157\,nF$; $C_T = 46,157\,nF$.

A PSpice simulation of the designed converter was made for different combinations of $\nu = [1,2; 1,3; 1,5; 1,8]$ and $R'_0 = [0,5; 1,0; 2,0; 3,0; 10; 100]$ (in real units corresponds to $R_0 = [19,83; 39,65; 79,31; 118,96; 396,53; 3965,32]\,\Omega$). The PSpice model circuit is shown on Fig. 4.

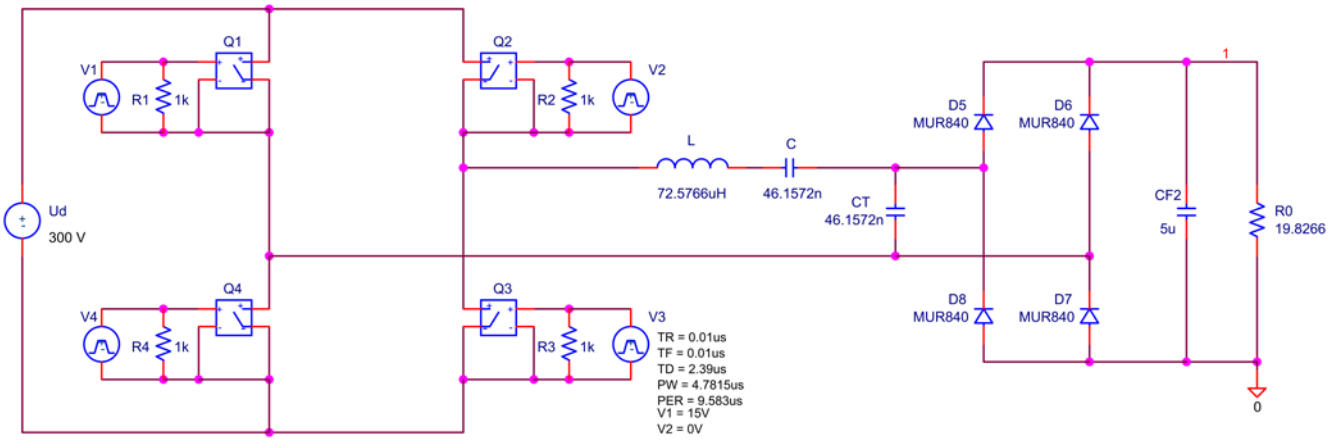

Fig. 4. PSpice simulation circuit of the designed LCC resonant DC/DC converter

The measured values of the output voltage (converted in relative units) are shown with points on Fig. 3. The results from the simulation together with these, obtained following the suggested methodology, are presented in Table I. The correspondence between the results is very good – the relative error is below 2%. It can be noticed that the error increases with the increase of the load resistor or the normalized switching frequency.

TABLE I
COMPARISON BETWEEN THE THEORETICAL AND SIMULATION RESULTS

		Simulation	Theory	Error
R'_0	ν	U'_0	U'_0	δ, [%]
0,5	1,2	1,044	1,044	0,049
	1,3	0,715	0,715	-0,026
	1,5	0,402	0,404	-0,434
	1,8	0,233	0,236	-1,214
1,0	1,3	1,422	1,422	-0,008
	1,5	0,743	0,746	-0,505
	1,8	0,383	0,388	-1,303
2,0	1,5	1,322	1,331	-0,671
	1,8	0,564	0,573	-1,443
3,0	1,5	1,800	1,815	-0,808
	1,8	0,669	0,679	-1,513
10	1,8	0,886	0,900	-1,577
100	1,8	0,992	1,004	-1,204

VI. CONCLUSION

A high-voltage LCC resonant DC/DC converter with capacitive output filter have been studied. It operates above the resonant frequency. In the proposed analysis the parasitic parameters of the matching transformer are taken into account. Typical operating modes of the converter are considered, according to the commutation time of the rectifier diodes. The control characteristics for each operating mode are obtained. The boundary curve between the modes, as well as the area of soft commutation of the transistors are presented in the plane of these characteristics.

The results of the theoretical study are compared with these of computer simulation using the software product OrCAD PSpice. The error between the obtained results is very small, less than 2%, which confirms the accuracy of the proposed methodology.

The described investigation can be used for designing LCC converter power supplies for microwave magnetrons, laser tubes, fluorescent lamps, etc. It is suitable especially for applications where a wide range of load changing is needed.

REFERENCES

[1] N. D. Madzharov, M. S. Gardevski, "A DC/DC High Voltage Power Supply", PCIM'10, Conference Proceeding, Nurnberg, Germany, 2010.

[2] N. D. Madzharov, "Autonomous Inverters with Energy Dosing for Ultrasonic Application", ICEST 2013, pp. 647-650, Ohrid, Macedonia, 2013.

[3] M. Rentzsch, F. Gleisberg, H. Güldner, F. Benecke and C. Ditmanson, "Closed Analytical Model of a 20 kV Output Voltage, 800 W Output Power Series-Parallel-Resonant Converter with Walton Cockroft Multiplier", PESC 2008. IEEE, pp. 1923-1929, 2008.

[4] J. Liu, L. Sheng, J. Shi, Z. Zhang and X. He, "Design of High Voltage, High Power and High Frequency Transformer in LCC Resonant Converter", APEC 2009, Twenty-Fourth Annual IEEE, pp. 1034-1038, Washington, USA, 2009.

[5] R. W. Erickson, D. Maksimovic, *Fundamentals of Power Electronics*, New York, Boston, Dordrecht, London, Moscow, Kluwer Academic Publishers, 2004.

[6] N. Bankov, A. Vuchev, Y. Madankov, "Analysis of High Voltage Resonance DC/DC Converter in Main Operating Mode", EICS 2013, pp. 224-229, Sofia, Bulgaria, 2013 (in Bulgarian).

[7] N. Bankov, A. Vuchev, Y. Madankov, "Analysis of High Voltage Resonance DC/DC Converter in Boundary Operating Mode", EICS 2013, pp. 230-235, Sofia, Bulgaria, 2013 (in Bulgarian).

[8] L. Rossetto, "A Simple Control Technique for Series Resonant Converters", IEEE Trans., Power Electronics, vol. 11, no. 44, pp. 554-560, 1996.

[9] N. D. Bankov, A. S. Vuchev, Y. K. Madankov, "Design Methodology for High Voltage Resonant DC/DC Converter for CO_2 Laser Power Supply", Annual Journal of Electronics, vol. 7, pp. 152-155, 2013.